Electronic Supplementary Material (ESI) for ChemComm.

Electronic Supporting Information

SANS study of mixed cholesteric cellulose nanocrystal – gold nanorod suspensions

Jonas Van Rie[a], Guillermo González-Rubio[b], Sugam Kumar[c#], Christina Schütz[a], Joachim Kohlbrecher[d], Michèle Vanroelen[e], Tom Van Gerven[e], Olivier Deschaume[f], Carmen Bartic[f], Luis M. Liz-Marzán[b,g], German Salazar-Alvarez[c] and Wim Thielemans[a,*]

a. Sustainable Materials Lab, Department of Chemical Engineering, KU Leuven, campus Kulak Kortrijk, Etienne Sabbelaan 53, 8500 Kortrijk, Belgium.
b. CICbiomaGUNE, Basque Research and Technology Alliance (BRTA), 20014 Donostia-San Sebastián, Spain
c. Department of Materials Science and Engineering, Ångström Laboratory, Uppsala University, Box 534, 751 21 Uppsala, Sweden
d. Laboratory for Neutron Scattering and Imaging, Paul Scherrer Institute, CH-5232 Villigen, Switzerland.
e. Department of Chemical Engineering, KU Leuven, Celestijnenlaan 200 F, 3001 Leuven, Belgium
f. Soft Matter and Biophysics Unit, Department of Physics and Astronomy, KU Leuven, Celestijnenlaan 200 D, 3001 Leuven, Belgium
g. Ikerbasque, Basque Foundation for Science

[#] Current address: Solid State Physics Division, Bhabha Atomic research Centre, Mumbai, 400 085, India

Experimental Section

CNC synthesis: Standard procedures were followed to obtain a cellulose nanocrystal suspension.[1] Cotton wool was hydrolysed in sulfuric acid (64 wt%) for 40 minutes at 45 ˚C. After centrifugation and dialysis, excess H^+ and OH^- ions were removed through mixing with Amberlite MB-6113 ion-exchange resin. A stable CNC suspension was subsequently obtained after removal of the resin by filtration. Excess water was evaporated under ambient conditions to a concentration of 10.6 wt%. This cellulose nanocrystal suspension was subsequently carefully diluted. To illustrate the development of the different phases as a function of cellulose nanocrystal concentration, a picture of 1-10 wt% CNC suspensions is shown in Figure SI-1. As can be seen in Figure SI1, macroscopic phase separation into an isotropic and chiral-nematic phase was observed for CNC concentrations of 5 wt% and higher. A Netzsch F3 Tarsus gravimetry instrument was used to determine the concentrations of CNC suspensions. The procedure involved heating of the samples to 85 ˚C at 10 ˚C per minute, with a subsequent isothermal period of 30 minutes, ending with another heating period at 10 ˚C per minute to a final 150 ˚C. The CNCs were furthermore characterized by atomic force microscopy (AFM) to have an average length of 185 ± 92 nm and width of 6.6 ± 2.4 nm.

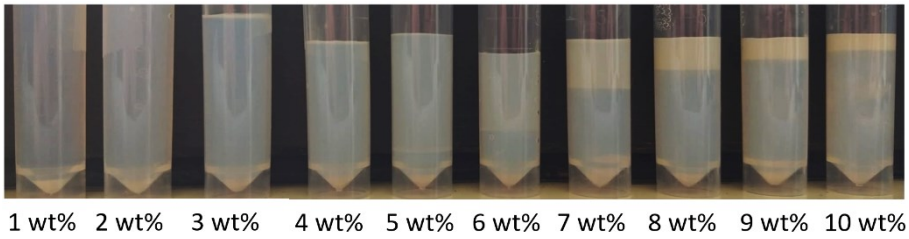

Figure S1. Cellulose nanocrystal suspensions. From 5 wt%, macroscopic phase separation is visible.

AuNR synthesis: AuNRs were synthesised based on the seed-mediated growth procedure described by Scarabelli *et al.*[2] All solutions were prepared with fresh milliQ water (18.2 MΩcm). *Seed solution.* Twenty five µl of a 0.05 M $HAuCl_4$ solution was added to 4.7 ml of a 0.1M CTAB solution at 30°C, turning the solution yellow. This was stirred at 300 rpm for 5 min. Next, a 10 mM $NaBH_4$ solution was freshly prepared and 300 µL of this solution was added while stirring at 1200 rpm, turning the colour of the seed brown. Stirring was reduced to 400 rpm after 20 seconds, and stopped after a couple of minutes *AuNR Growth:* 900 mg CTAB was dissolved in 50 ml milliQ water at 30°C. After the solution turned completely transparent, 50 mg 5-bromosalicylic acid was added while stirring slowly. When everything was dissolved, 480 µl of a 0.01 M $AgNO_3$ solution was added under stirring at 300 rpm. This solution was stirred for another 15 minutes at 300 rpm, after which 500 µl of a 0.05 M $HAuCl_4$ solution was added. This quickly turned the solution dark orange. The solution was further stirred at 300 rpm during 1 hour and the colour slowly evolved towards light yellow (until the absorption intensity of the peak at 390 nm decreased to 0.5-0.6 as measured in a cuvette of optical pathlength of 1 cm). Next, 130 µl of a 17.4 mg/mL ascorbic acid solution was added while stirring at 1200 rpm. Upon addition, the colour of the solution turned almost immediately transparent. 80 µL of a freshly prepared seed solution was quickly added while stirring at 1200 rpm. After 30 seconds, stirring was stopped and the solution was left to grow for a couple of hours. Finally, The AuNRs were centrifuged for 30 minutes at 6000 rpm. The gold concentration in the aqueous phase was measured by Inductively Coupled Plasma Mass Spectrometry (ICP-MS, Perkin Elmer ELAN DRC-e). Aqueous samples were diluted in 10 mL 2 % HNO_3 and Lutetium was used as an internal standard. If intermediate dilutions were required, Yttrium was added as a second internal standard to check the consistency of these dilutions. The dimensions of the AuNRs were determined by AFM, which gave an average length of 62 ± 4.8 nm and average width of 20.4 ± 3.3 nm.

AuNR-CNC system. AuNR solutions of different concentrations (i.e., 0.0014, 0.007 and 0.021 wt%) were mixed with the aqueous CNC suspensions (1, 3, 5, 8 and 10.6 wt%) and dialysed against mixtures of water and deuterated water. Dialysis tubes were filled with 1 mL of each sample, and left to dialyse in 10 mL of a D_2O:H_2O mixture. After two days, the mixture of D_2O:H_2O mixture was refreshed. A 35:65 D_2O:H_2O mixture was used to prepare the suspension with the solvent contrast matched to CNCs in the assembly and for the independent visualisation of the AuNRs.[3] A 72:28 D_2O:H_2O mixture was used to match the solvent to AuNRs and visualize the CNCs in the AuNR-CNC solutions.[4] Pure CNC suspensions (references) were dialysed against pure D_2O.

Characterization Techniques

SANS experiments: SANS spectra were recorded on the SANS-II instrument at the Swiss spallation neutron source SINQ, Paul Scherrer Institute, Villigen, Switzerland**.**[5] The samples were measured at a 6 m sample-detector distance, lambda 0.73 nm and a 3 m sample-detector distance, lambda 0.55. The set-up had a ^{3}He detector with 128x128 pixels. One mm path length quartz glass capillaries were used for all measurements. The samples were loaded in a sample holder and measured in the same run. Based on standard procedures, all obtained data were calibrated for detector nonlinearity using the incoherent scattering from 1 mm thick D_2O samples. The scanned q-range was $0.01 \leq q \leq 1$ nm^{-1} to study the arrangement of gold nanoparticles in the CNC matrix.[6,7] BerSANS software was used to subtract dark background due to electronic noise/stray neutrons and the background due to the sample environment to obtain the scattering signal of the sample. BerSANS was furthermore used for initial data reduction and to obtain values for the transmissions of all measured samples.[8] Further data reduction was done using GRASP software (a Matlab™ script developed by Institut Laue-Langevin for analysis and reduction of data produced by SANS experiments) to obtain the final 1D scattering patterns.

AFM characterization

*CNCs***:** On a freshly by scotch-tape cleaved mica surface (NanoAndMore GMBH) 20 µL poly-L-lysine solution (Sigma Aldrich, 0.1% w/v in water) was deposited for 3 minutes, subsequently rinsed with deionized water and dried with compressed air. Following, 20 µL of a CNC dispersion (0.001 wt%) was placed on the treated surface for 3 minutes, then rinsed with deionized water and dried with compressed air. The sample were left in a vacuum oven at 40°C overnight. A Multi-mode V AFM (Digital instruments Nanoscope Veeco) was used in tapping mode and AFM probes from Budget Sensors (Tap300 Al-G, resonance frequency 300 kHz and force constant 40 N/M) were used to image the samples. The length of 300 particles was measured manually using imageJ[9] and the mean length and standard deviation as well as a log-normal distribution were determined. The width was extracted as the height for at least 450 points on representative particles.

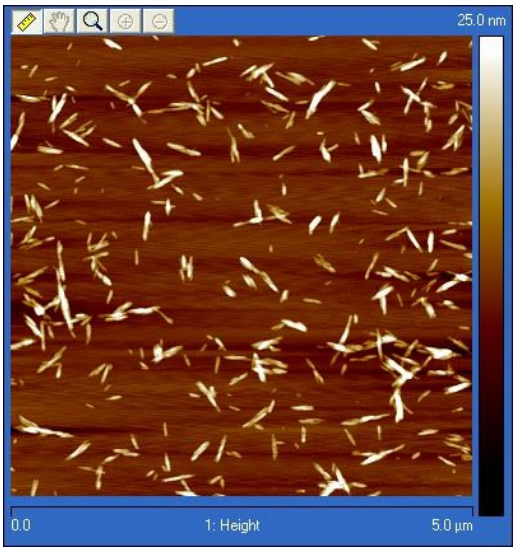

Figure S2.1 AFM images of CNCs.

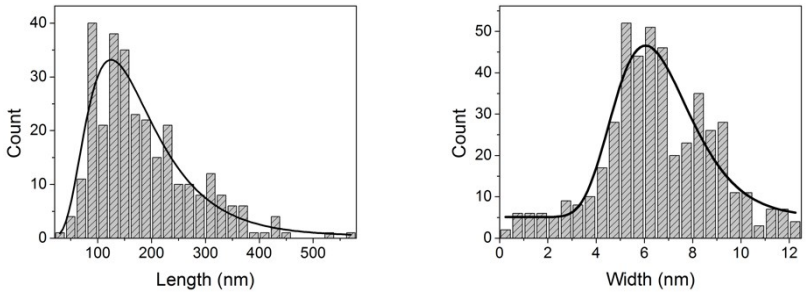

Figure S2.2. Histogram of the length (left) and width (right) distributions of CNCs measured from AFM images.

AuNRs. An Agilent 5500 AFM system with MSNL-F cantilevers (f = 110=120 kHz, k = 0.6 N/m, average tip radius of 2=12 nm) was used for topographical imaging of the particles in intermittent contact (AAC) mode. The AFM topography images were leveled, line-corrected and measured (height profiles) using Gwyddion,[10] a free and open-source SPM (scanning probe microscopy) data visualization and analysis program.

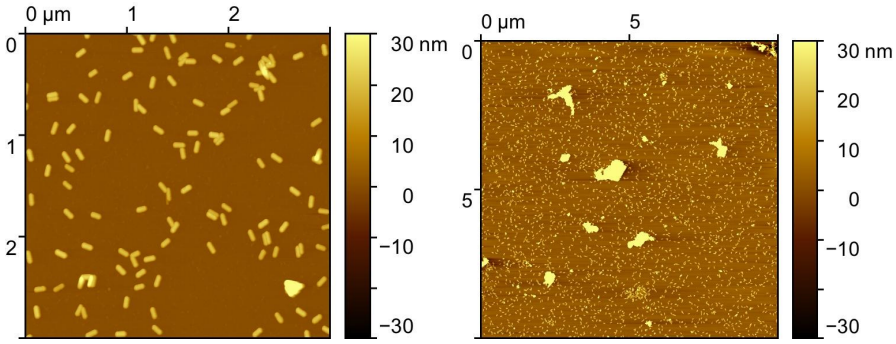

Figure S 3.1. AFM images of AuNRs.

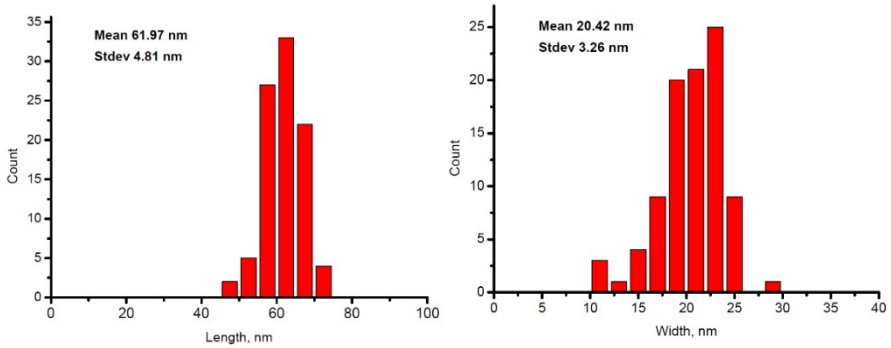

Figure S3.2. Mean length (left) and width (right) histograms of AuNRs.

TEM characterization of AuNR-CNC: Low magnification TEM images were obtained with a JEOL JEM-1400PLUS transmission electron microscope, operating at an acceleration voltage of 120 kV. Carbon-coated 400 square mesh copper grids were used.

SANS Data Analysis:

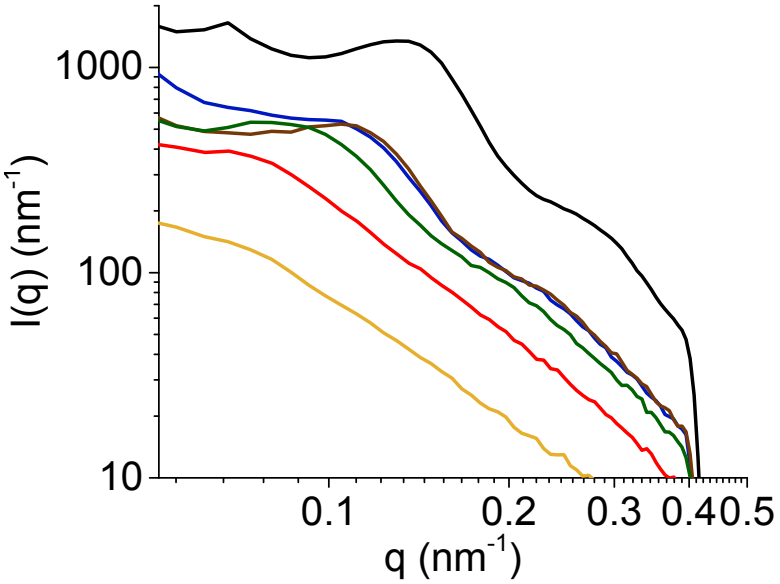

Figure S4.1. SANS curves showing the evolution of CNC scattering data at fixed AuNR concentration (0.0014 wt%) for AuNR-CNC assemblies in the isotropic (upper) phase, containing 1 (orange), 3 (red), 5 (green), 8 (blue) and 10.6 (brown) wt% CNCs. An 8 (black) wt% CNC reference SANS curve is also shown.

SANS curves with Lorentz fits and Kratky representations

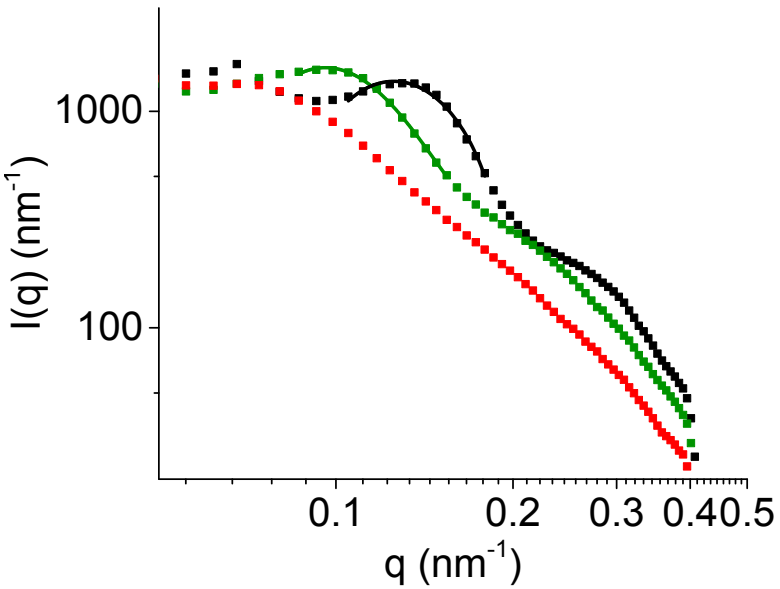

Figure S4.2. SANS curves and Lorentz fits of 3 (red), 5 (green) and 8 (black) wt% CNC suspensions.

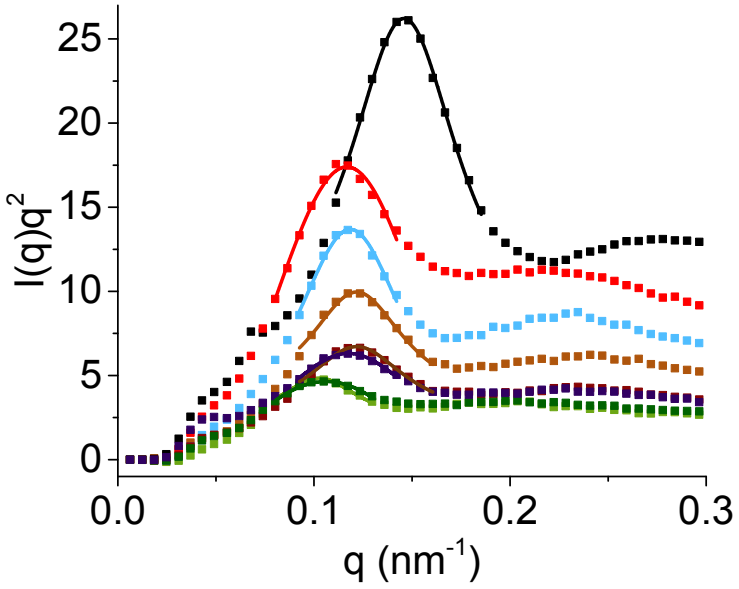

Figure S4.3. Kratky plots and Lorentz fits of the AuNR-CNC systems (matching for gold) containing 5 (green), 8 (blue) and 10.6 (brown) wt% CNCs and 0.0014 wt% AuNRs (dark green, blue and brown curves represent the isotropic phase; light green, blue and brown curves the chiral nematic phase). Five (red) and 8 (black) wt% CNC curves in the absence of AuNRs are shown for comparison.

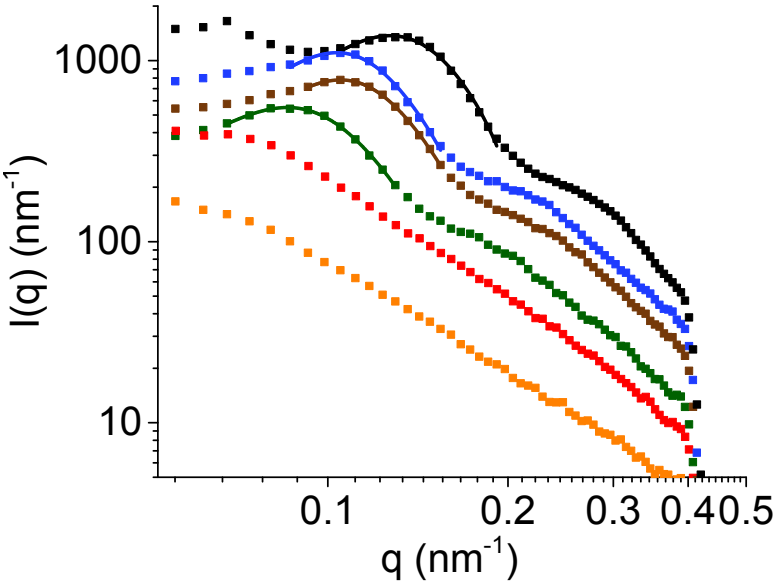

Figure S4.4. SANS plots of the AuNR-CNC systems in the nematic liquid crystalline phase (matching for gold) containing 1 (orange), 3 (red), 5 (green), 8 (blue) and 10.6 (brown) wt% CNCs and 0.0014 wt% AuNRs, showing Lorentz fits. An 8 (black) wt% CNC curve in the absence of AuNRs is shown for comparison.

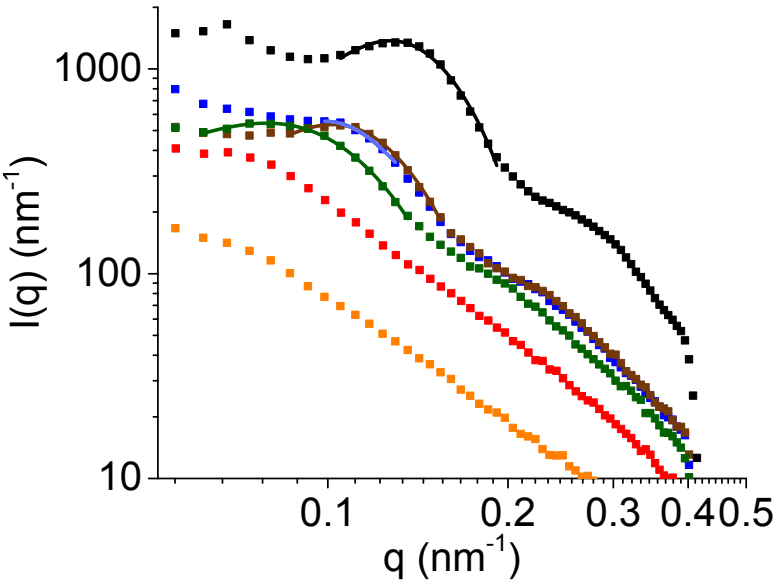

Figure S4.5. SANS plots of the AuNR-CNC systems in the isotropic phase (matching for gold) containing 1 (orange), 3 (red), 5 (green), 8 (blue) and 10.6 (brown) wt% CNCs and 0.0014 wt% AuNRs, showing Lorentz fits. An 8 (black) wt% CNC curve in the absence of AuNRs is shown for comparison.

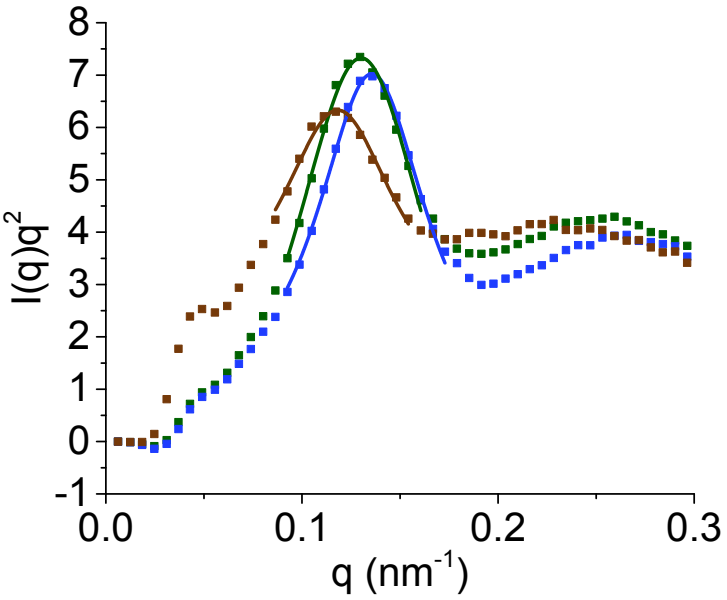

Figure S4.6. Kratky plots of the AuNR-CNC systems (matching for gold) containing 0.0014 (brown), 0.007 (green) and 0.021 (blue) wt% of AuNRs and 8 wt% of CNCs, showing Lorentz fits.

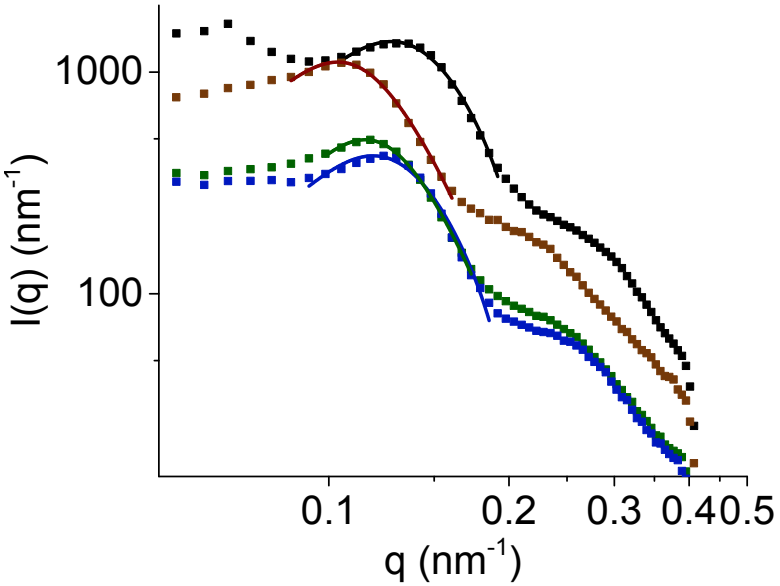

Figure S4.7. SANS plots of the AuNR-CNC systems (matching for gold) containing 0.0014 (brown), 0.007 (green) and 0.021 (blue) wt% of AuNRs and 8 wt% of CNCs, showing Lorentz fits. An 8 (black) wt% CNC curve in the absence of AuNRs is shown for comparison.

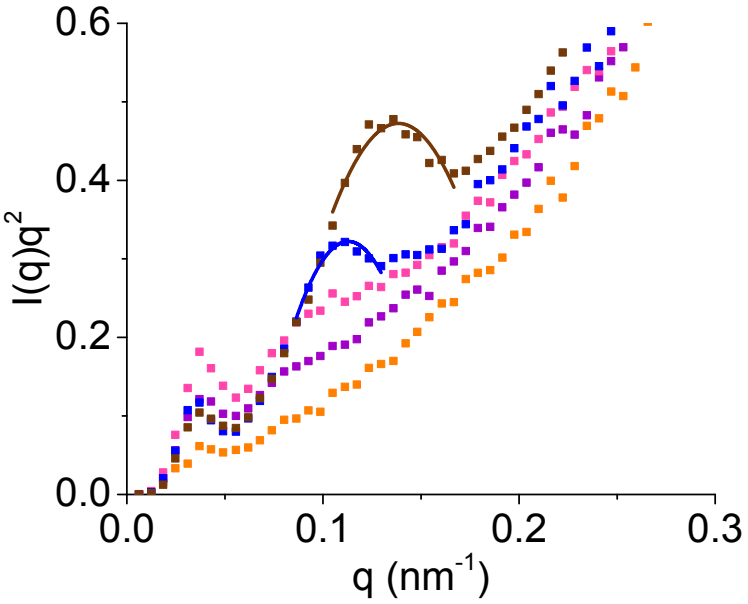

Figure S4.8. Kratky plots of the AuNR-CNC systems (matching for CNCs) containing 1 (orange), 3 (purple), 5 (pink), 8 (blue) and 10.6 (brown) wt% CNCs and 0.0014 wt% AuNRs, showing Lorentz fits.

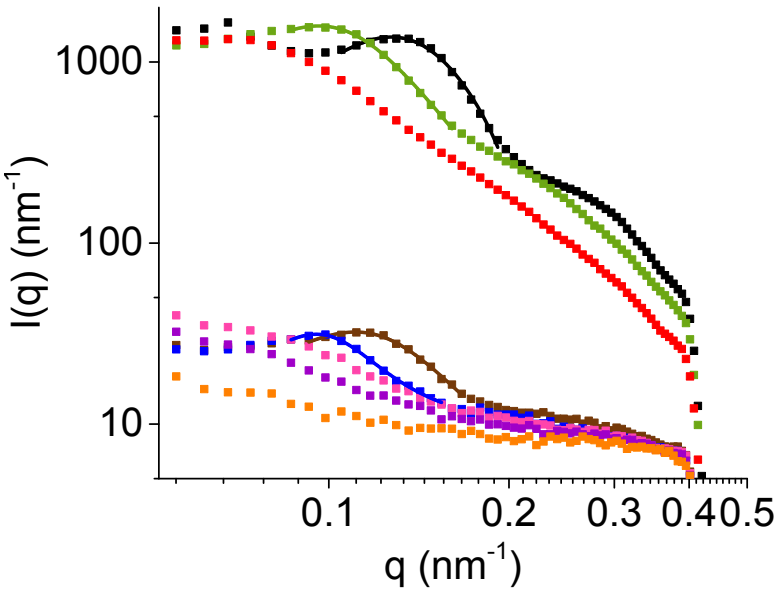

Figure S4.9. Kratky plots of the AuNR-CNC systems (matching for CNCs) containing 1 (orange), 3 (purple), 5 (pink), 8 (blue) and 10.6 (brown) wt% CNCs and 0.0014 wt% AuNRs, showing Lorentz fits. Three (red), 5 (green) and 8 (black) wt% CNC curves in the absence of AuNRs are shown for comparison.

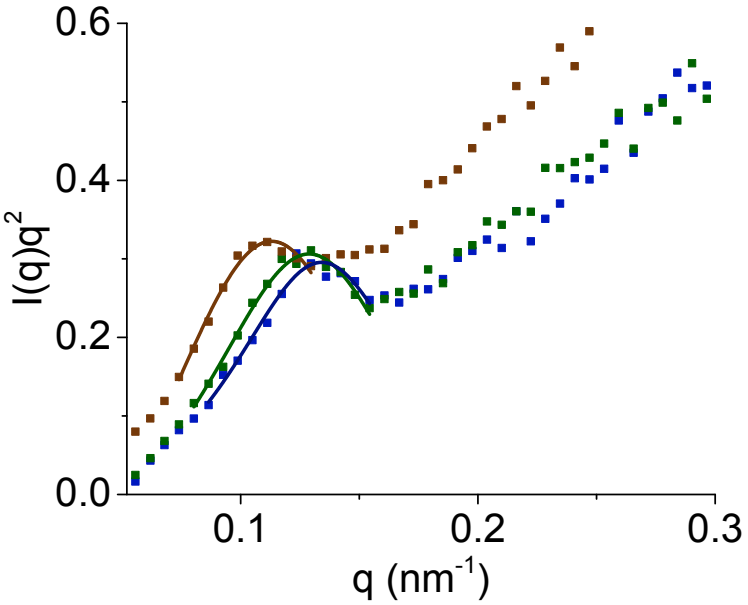

Figure S4.10. Kratky plots of the AuNR-CNC systems (matching for CNCs) containing 0.0014 (brown), 0.007 (green) and 0.021 (blue) wt% AuNRS and 8 wt% CNCs, showing Lorentz fits.

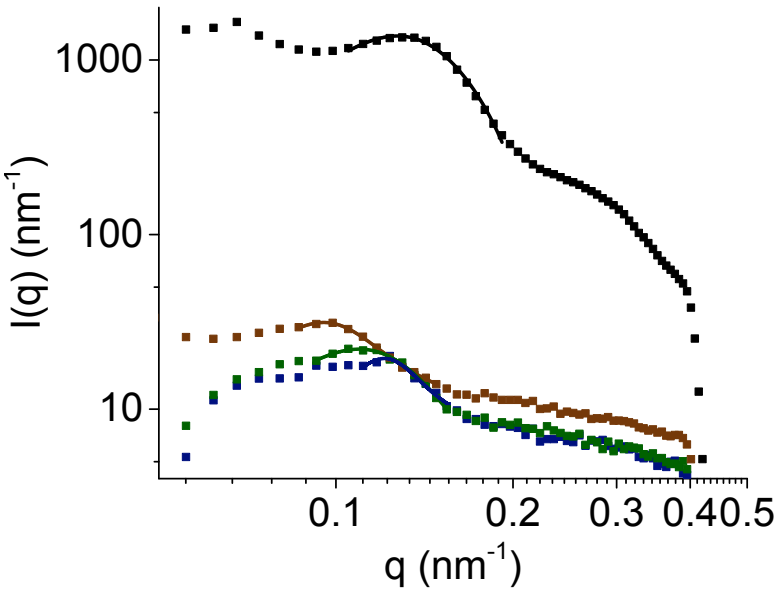

Figure S4.11. SANS plots of the AuNR-CNC systems (matching for CNCs) containing 0.0014 (brown), 0.007 (green) and 0.021 (blue) wt% AuNRS and 8 wt% CNCs, showing Lorentz fits. An 8 (black) wt% CNC curve is shown for comparison.

Correlation distances

Table S1.1. Correlation distances obtained from a Lorentz fit of the structure peak of AuNR-CNC systems containing 1-10.6 wt% of CNCs and 0.0014 wt% of AuNRs. The correlation distance reduces as the CNC concentration increases.

CNC conc. (wt%)	AuNR conc. (wt%)	q_{max} (nm^{-1}) *Ch. nem. phase*	St. dev. (nm^{-1})	d (nm) *Ch. nem. phase*	q_{max} (nm^{-1}) *Iso. phase*	St. dev. (nm^{-1})	d (nm) *Iso. phase*
8	-	0.14593	0.00026	43	-		-
5	0.0014	0.10268	0.00056	61	0.10644	0.00066	59
8	0.0014	0.11852	0.00046	53	0.11757	0.00052	53
10.6	0.0014	0.12174	0.00060	52	0.12168	0.00043	52

Table S1.2. Correlation distances obtained from a Lorentz fit of the structure peak of AuNR-CNC systems containing 0.0014-0.021 wt% of AuNRs and 8 wt% of CNCs.

CNC conc. (wt%)	AuNR conc. (wt%)	q_{max} (nm^{-1})	St. dev. (nm^{-1})	d (nm)
8	-	0.14593	0.00026	43
8	0.0014	0.11826	0.00060	53
8	0.007	0.13015	0.00036	48
8	0.021	0.13562	0.00026	46

Table S1.3. Correlation distances obtained from a Lorentz fit of the structure peak of AuNR-CNC containing 1-10.6 wt% of CNCs and 0.0014 wt% of AuNRs.

CNC conc. (wt%)	AuNR conc. (wt%)	q_{max} (nm^{-1})	St. dev. (nm^{-1})	d (nm)
8	-	0.14593	0.00026	43
8	0.0014	0.11288	0.00110	56
10.6	0.0014	0.13843	0.00147	45

Table S1.4 Correlation distances obtained from a Lorentz fit of the structure peak of Au-CNC containing 0.0014-0.021 wt% of AuNRs and 8 wt% of CNCs.

CNC conc. (wt%)	AuNR conc. (wt%)	q_{max} (nm^{-1})	St. dev. (nm^{-1})	d (nm)
8	-	0.14593	0.00026	43
8	0.0014	0.11302	0.00099	56
8	0.007	0.12882	0.00070	49
8	0.021	0.13409	0.00139	47

SANS data of the isotropic and nematic phases. Comparison of SANS curves obtained from the isotropic and nematic phases of the AuNRs and CNCs mixtures.

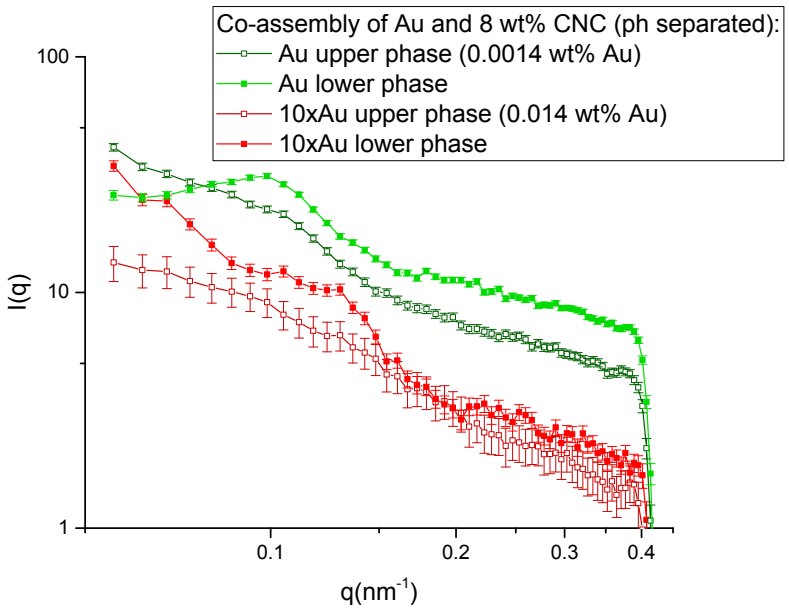

Figure S5. SANS curves of Au-CNC assemblies containing 8 wt% CNCs and 0.014 wt% AuNRs (red curves), 0.0014 wt% AuNRs (green curves). A comparison of the upper (isotropic) and lower (cholesteric) phases are shown. The influence of the concentration of gold nanorods on the position of the structure peak is also clearly visible.

Summary of correlation distances of CNCs and AuNRs in the assemblies as function of concentrations.

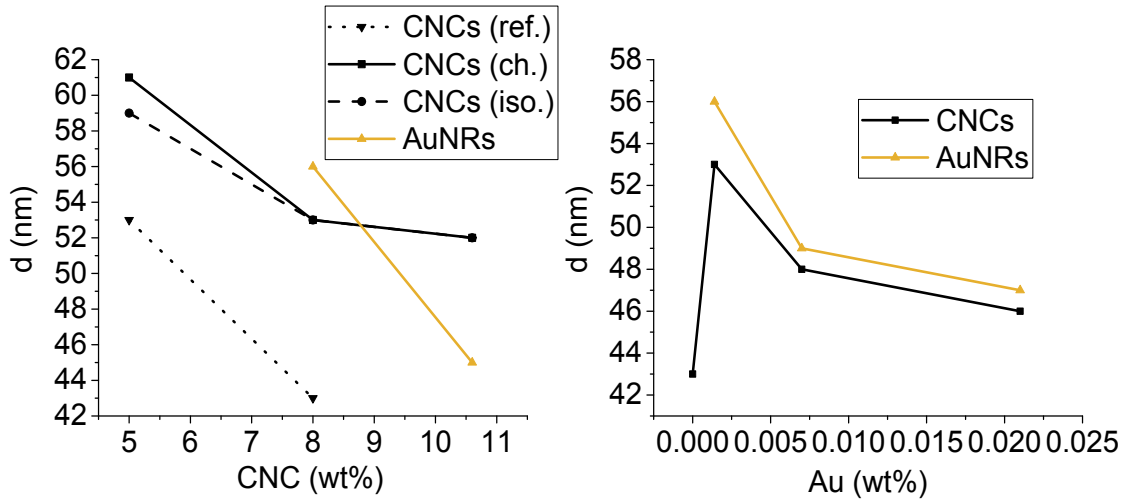

Figure S6. Evolution of the correlation distances between AuNRs and CNCs in the investigate AuNR-CNC systems as a function of the CNC (left) and AuNR (right) concentrations.

References

1 L. Jasmani, S. Eyley, R. Wallbridge and W. Thielemans, *Nanoscale*, 2013, **5**, 10207–11.

2 L. Scarabelli, A. Sánchez-Iglesias, J. Pérez-Juste and L. M. Liz-Marzán, *J. Phys. Chem. Lett.*, 2015, **6**, 4270–4279.

3 M. Martínez-Sanz, M. J. Gidley and E. P. Gilbert, *Soft Matter*, 2016, **12**, 1534–1549.

4 G. Nyström, M. P. Fernández-Ronco, S. Bolisetty, M. Mazzotti and R. Mezzenga, *Adv. Mater.*, 2016, **28**, 472–478.

5 P. Strunz, K. Mortensen and S. Janssen, *Phys. B Condens. Matter*, 2004, **350**, E783–E786.

6 M. Uhlig, A. Fall, S. Wellert, M. Lehmann, S. Prévost, L. Wågberg, R. von Klitzing and G. Nyström, *Langmuir*, 2016, **32**, 442–450.

7 C. Schütz, M. Agthe, A. B. Fall, K. Gordeyeva, V. Guccini, M. Salajková, T. S. Plivelic, J. P. F. Lagerwall, G. Salazar-Alvarez and L. Bergström, *Langmuir*, 2015, **31**, 6507–6513.

8 U. Keiderling, *Appl. Phys. A Mater. Sci. Process.*, 2002, **74**, s1455–s1457.

9 C. A. Schneider, W. S. Rasband and K. W. Eliceiri, *Nat. Methods*, 2012, **9**, 671–675.

10 D. Nečas and P. Klapetek, *Cent. Eur. J. Phys.*, 2012, **10**, 181–188.